

Transient interference of transmission and incidence

A. L. Pérez Prieto,¹ S. Brouard,¹ and J. G. Muga²

¹*Departamento de Física Fundamental II, Universidad de La Laguna, La Laguna, Spain*

²*Departamento de Química-Física, Universidad del País Vasco, Apartado 644, 48080 Bilbao, Spain*

(Received 9 May 2000; published 7 June 2001)

Due to a transient quantum interference during a wave packet collision with a potential barrier, a particular momentum, that depends on the potential parameters, but is close to the initial average momentum, becomes suppressed. The hole left pushes the momentum distribution outwards leading to a significant constructive enhancement of lower and higher momenta. This is explained in the momentum complex-plane language in terms of a saddle point and two contiguous “structural” poles, which are not associated with resonances but with incident and transmitted components of the wave function.

DOI: 10.1103/PhysRevA.64.012710

PACS number(s): 03.65.Nk, 11.55.-m

In the traditional exposition of quantum-scattering theory, it is assumed that only the *results* of the collision, unlike the collision itself, can be observed at “asymptotic” distances and times. Indeed, in standard collision experiments with atomic or molecular beams, only the asymptotic results are observed. However, in modern experiments the collision complex is observed by means of femtosecond laser pulses or “spectroscopy of the transition state” [1]. Also, in quantum kinetic theory of gases, accurate treatments must abandon the “completed collision” approximation and use a full description, e.g., in terms of Möller wave operators as in the Waldmann-Snyder equation and its generalizations for moderately dense gases [2]. In any case, it is important to understand the whole collision process to control or modify the products. This has motivated a recent trend of theoretical and experimental work to investigate the collision itself, and not only its asymptotics. In particular, a quantum effect has been recently described by Brouard and Muga [3,4] in which the probability to find the particle with a momentum above a given value is larger, in the midst of the collision, than the quantity allowed classically by energy conservation. The effect belongs to a group where the conservation of energy seems to be violated from a classical perspective. Well-known examples are the tunnel effect, or in general, the non-vanishing probability to find the particle in evanescent regions beyond the classical turning points.

The transient enhancement of the momentum tail may, in principle, be observed by colliding ultracold atoms with a laser field that is turned off suddenly in the time scale of the atomic motion [3]. Moreover the effect implies deviations from the Maxwellian velocity distribution as a macroscopic consequence [5].

We initiated the research that has led to the present work, looking for conditions that increase the effect and favor its observability. In doing so we have found an unexpected regime where the enhancement is much higher than in previously studied cases. In this article we shall describe such a regime and analyze its physical origin, namely, a transient interference between transmission and incidence components of the wave packet ψ .

Let us first briefly review the main aspects of the classically forbidden increase of high momenta. Brouard and Muga have studied several examples of one-dimensional collisions where the quantity

$$G^q(p,t) \equiv \int_p^\infty \{|\psi(p',t)|^2 - |\psi(p',0)|^2\} dp'$$

takes on positive values for positive potentials (the corresponding classical quantity is negative or zero due to energy conservation) [3,4]. An important aspect of this effect is its *transient* character, $G^q \leq 0$ before and after the collision. The effect is also *generic* [3,4] because the stationary components of the wave packet have, in momentum representation, a tail due to the resolvent that is always present in the Lippmann-Schwinger equation. This tail goes beyond the maximum value allowed by the conservation of energy.

For a Gaussian wave packet colliding with an infinite wall, maximum values of $G_{max}^q(p,t) \approx 0.05$ have been reported [3]. Also a “ δ ” potential was used [4] to analyze the influence of the opacity of the barrier. For the cases examined, an increase of G^q with the opacity was observed up to a saturation level where the infinite wall results were recovered [4]. This suggested that the observability of the effect would improve with strongly opaque conditions. In a complementary study we have systematically varied the spatial variance of the wave packet, δ_x , and the height of a square barrier, V_0 , for a fixed average initial momentum p_c . Contrary to previous expectations, the maximum effect corresponds to energies well above the barrier and to large values of δ_x . In this regime, where we have found values of G_{max}^q as large as 0.37, the barrier is not at all opaque and essentially the full wave is finally transmitted.

The numerical effort to perform these calculations by ordinary propagation methods (such as the split-operator method) is rather heavy, since large values of δ_x and the need to discern fine details of the momentum distribution require an extense and dense grid. In fact for very large values of δ_x this numerical route has to be eventually abandoned. But even if one gets numerical results with enough computer power, they will not provide any explanation of the unexpectedly high G^q values. Fortunately these two difficulties can be overcome with an approximate analytical solution. Its obtention follows Ref. [6] closely. First the momentum representation of the wave function is expressed using the basis of stationary eigenstates of H , $|p'^+\rangle$, corresponding to incident momentum p' , and energy $E' = p'^2/(2m)$,

$$\psi(p,t) = \int_{-\infty}^{+\infty} \langle p|p'^+\rangle e^{-iE't/\hbar} \langle p'^+|\psi(t=0)\rangle dp'. \quad (1)$$

If the initial state at time $t=0$ does not overlap with the potential and has negligible negative momentum components we can write

$$\psi(p,t) = \int_0^{+\infty} \langle p|p'^+\rangle e^{-iE't/\hbar} \langle p'^+|\psi(t=0)\rangle dp'. \quad (2)$$

To facilitate the treatment of the integral in the p' -complex plane we may now extend the lower limit to $-\infty$ using the analytical continuation of $\langle p|p'^+\rangle$, $p' > 0$, over $p' < 0$ (and later over the whole complex plane).

For a barrier between $-d/2$ and $d/2$, the δ -normalized stationary wave functions with incident momentum p' have the form

$$\langle x|p'^+\rangle = \frac{1}{h^{1/2}} \begin{cases} Ie^{ip'x/\hbar} + Re^{-ip'x/\hbar}, & x < -d/2 \\ \chi(x;p'), & -d/2 < x < d/2 \\ Te^{ip'x/\hbar}, & x > d/2, \end{cases} \quad (3)$$

where $I=1$ and R and T are the reflection and transmission amplitudes, respectively. The momentum representation $\langle p|p'^+\rangle$ will have four terms corresponding to I , R , χ , and T . The terms with I , R , and T have *structural poles* [7] in the p' -complex momentum plane at

$$p'_I = p + i0, \quad (4)$$

$$p'_R = -p - i0,$$

$$p'_T = p - i0,$$

which are not related to resonances or to the potential profile. The functions R and T may present *resonance and antiresonance poles* in the third and fourth quadrants. However, the conditions examined in this work correspond to “direct scattering,” where these resonance singularities do not play any significant role.

The initial state is taken as a minimum-uncertainty-product Gaussian centered at the position $-\alpha\delta_x$, $\alpha > 0$, with average momentum p_c ,

$$\langle p'|\psi(t=0)\rangle = \left(\frac{2\delta_x}{\pi\hbar^2}\right)^{1/4} \exp\left[-\frac{\delta_x(p'-p_c)^2}{\hbar^2} + \frac{ip'\alpha\delta_x}{\hbar}\right]. \quad (5)$$

This expression and the momentum representation of Eq. (3) are inserted in Eq. (2) to obtain four integrals. For the cases discussed in this article, however, only two of them associated with incident and transmitted components, are relevant, and will be studied in detail. We may neglect the contribution of χ , since the wave is much more extended in space than the barrier, and we may also neglect the reflection term,

since the collision takes place well above the barrier top. The validity of these approximations is confirmed by our numerical calculations.

The remaining contribution is

$$\psi_{IT} = ih^{-1/2}\hbar\tau \int_{-\infty}^{\infty} [g_I(p') + g_T(p')] e^{\phi(p')} dp', \quad (6)$$

where

$$\tau = \frac{1}{\sqrt{2\pi\hbar}} \left(\frac{2\delta_x}{\pi\hbar^2}\right)^{1/4},$$

$$g_I(p') = \frac{e^{ip'd/2\hbar}}{p-p'+i0},$$

$$g_T(p') = \frac{-T(p')\exp[i(2p'-p)d/2\hbar]}{(p-p'-i0)},$$

and

$$\phi(p') = \frac{-ip'^2t}{2m\hbar} - \frac{\delta_x(p'-p_c)^2}{\hbar^2} + \frac{ip'(\alpha\delta_x - d/2)}{\hbar}. \quad (7)$$

The functions $g_I(p')$ and $g_T(p')$ present structural poles at p'_I and p'_T , respectively; in addition, $g_T(p')$ may have resonance and antiresonance poles.

The steepest descent path (SDP) is a straight line with negative slope $-t\hbar/(2m\delta_x)$, and with a saddle point close to p_c in the midst of the collision at

$$s = \frac{m}{4m^2\delta_x^2 + t^2\hbar^2} \{4mp_c\delta_x^2 + (\alpha\delta_x - d/2)\hbar^2 t + i2\hbar[m\delta_x(\alpha\delta_x - d/2) - p_c\delta_x t]\}. \quad (8)$$

We shall always assume that the slope is small enough so that when the integration contour is deformed along this path it “cuts” the resonance poles of the fourth quadrant far from the real axis, so that their residues can be neglected (“direct scattering” conditions).

To evaluate the integral in Eq. (6), the contour is deformed to the SDP passing over the saddle. Because of the interference between the saddle and the structural poles, it is necessary to find a uniform expression for a smooth treatment of the crossing of the pole by the SDP. This is provided by the w function, $w(z) = e^{-z^2} \operatorname{erfc}(-iz)$, which may also be defined by its integral expression [8]

$$w(z) = \frac{1}{i\pi} \int_{\Gamma_-} du \frac{e^{-u^2}}{u-z}, \quad (9)$$

where Γ_- goes from $-\infty$ to ∞ passing below the pole.

To introduce the w functions, the integrand must be put in the form of Eq. (9). We complete the square in Eq. (7) and use the change of variable

$$u = \frac{p' - s}{f}, \quad f = \left(\frac{\delta_x}{\hbar^2} + i \frac{t}{2m\hbar} \right)^{-1/2} \quad (10)$$

to obtain

$$\begin{aligned} \langle p | \psi(t) \rangle &\approx i f \tau \hbar^{-1/2} \exp[-(\delta_x p_c^2 / \hbar^2) + \eta^2] \\ &\times \int_{-\infty}^{\infty} [g_I(u) + g_T(u)] e^{-u^2} du, \end{aligned}$$

where $g(u) \equiv g(p'(u))$, and

$$\eta = \left(\frac{2p_c \delta_x}{\hbar^2} + i \frac{(\alpha \delta_x - d/2)}{\hbar} \right) \left[4 \left(\frac{\delta_x}{\hbar^2} + i \frac{t}{2m\hbar} \right) \right]^{-1/2}.$$

The main contribution from g_I is retained by approximating $g_I(u) \approx \mathcal{R}_I / (u - u_I)$, where \mathcal{R}_I is the residue of $g_I(u)$ at the point $u = u_I = (p'_I - s)/f$. Finally, proceeding similarly for g_T ,

$$\begin{aligned} \langle p | \psi(t) \rangle &\approx h^{-1/2} \pi \tau \hbar \exp[-(\delta_x p_c^2 / \hbar^2) + \eta^2] \\ &\times e^{i p d / 2 \hbar} [w(u_I) + T(p)w(-u_T)] \\ &\equiv \psi_{IT}^0(p, t). \end{aligned} \quad (11)$$

As a test of consistency, let us consider the limit $d \rightarrow 0$ of this expression. Since $u_I \approx u_T$, by taking into account the relation between w functions with argument of opposite sign, see Eq. (9),

$$w(u_I) = e^{-u_I^2} - w(-u_T), \quad (12)$$

it follows that $\langle p | \psi(t) \rangle$ goes to $\langle p | \psi(0) \rangle$ as $d \rightarrow 0$, as expected. Note that there is not a simple uncertainty type of relation between the momentum spread (or the importance of the effect) and d , since the barrier, unlike the diaphragm of the Heisenberg's microscope, does not limit the wave packet size to the value d . In fact, as d goes to zero, the width in momentum space remains constant.

More precise expressions including reflection and χ terms may be obtained for specific models. In particular, we have worked out analytical corrections to the zeroth order ψ_{IT}^0 for the square barrier [9], which allow to obtain the wave function and G_{max}^q accurately for large values of δ_x with small computational effort. However, Eq. (11) is generic, it captures the essential and provides a simple and explanatory picture of the phenomenon we want to discuss. One may be tempted to try a further simplification and use a Born approximation for $T(p)$ in Eq. (11). However, for the cases studied the energy where the maximum effect takes place is not sufficiently large [$|T(p)|_{Born}^2 / |T(p)|^2 \approx 200$ in the example discussed below].

Figure 1 shows the distribution of momenta $|\langle p | \psi(t) \rangle|^2$ for different instants of time, from the initial one to a time after the collision with a square barrier has been completed, passing through the instant for which $G^q = 0.27$ is maximum for this particular collision. In all figures, the numerical val-

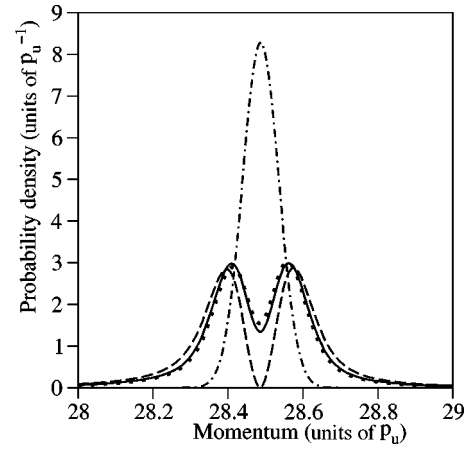


FIG. 1. $|\langle p | \psi(t) \rangle|^2$ for different values of t : $t=0$ (dotted-dashed line); $t=2.333t_u$ (solid line); $t=2.731t_u$ (dashed line); and $t=3.233t_u$ (dotted line). $m=1.558023m_u$, $V_0=102.5e_u$, $d=2.5l_u$, $-\alpha\delta_x=-50l_u$, $\delta_x=107.99l_u^2$, with an average momentum $p_c=28.48p_u$ well above the classical threshold $(2mV_0)^{1/2}=17.87p_u$. The units are scaled for numerical convenience in the computations as $e_u=10^{-13}$ a.u. of energy, $p_u=10^{-4}$ a.u. of momentum, $l_u=10^4$ a.u. of length, $m_u=10^3$ a.u. of mass, and $t_u=10^{13}$ a.u. of time.

ues are chosen for collisions of ultracold Rubidium atoms with an effective ‘‘laser’’ barrier. The observed behavior does not have a classical explanation. Recall that the wave packet is considerably broader than the barrier. Thus, a classical ensemble of particles with the same Gaussian phase-space (Wigner) distribution as in Eq. (5) would only be slightly deformed due to the small fraction of particles located on the barrier top at a given time, and would keep the maximum at the average momentum p_c . Moreover, there could not be any spectacular acceleration or deceleration as the one seen in the two peaks of the quantum distribution. We shall see that the zero of the quantum momentum distribution, which forbids in this case the initially dominant momentum p_c , is due to a destructive interference, whereas the two new peaks correspond to momentum regions of constructive interference.

In Fig. 2 the *Argand diagrams* of the two terms of Eq. (11) are represented, namely, the imaginary versus the real parts of incident and transmission components, obtained by varying p at equal intervals. Each lobule corresponds to one of the terms. The ‘‘motion’’ as p increases begins close to the origin, downwards in both diagrams. The left peak of the momentum distribution, see Fig. 1, corresponds to the zone where the two moduli increase together and are approximately in phase. After the descending motion there is a fast, approximately circular motion where the phases become opposed (destructive interference). Finally, the two curves meet again *in phase* in the upper part of the lobules, this momentum interval corresponds to the right peak of the momentum distribution. The described behavior is essentially due to the two w functions, $w(u_I)$ and $-w(-u_T)$. The phase opposition alone does not explain, however, why the interference is totally destructive. It is also necessary that the incidence and transmission terms of Eq. (11) have equal moduli for an

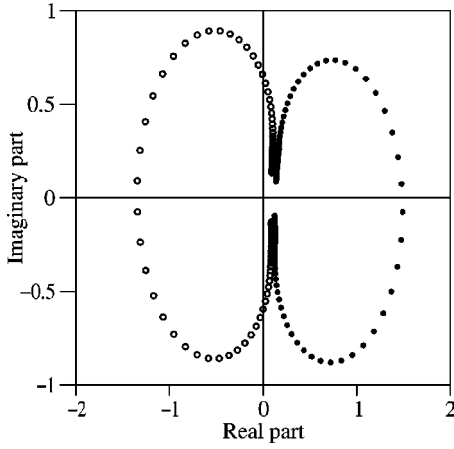


FIG. 2. Imaginary versus real parts of the incident contribution to $\psi_{IT}^0(p,t)$ (empty circles), and of the transmission contribution (filled circles), for $t=2.731t_u$ and different values of p equally spaced between $p=28p_u$ and $p=29p_u$. Other parameters as in Fig. 1.

exact cancellation. Actually, the equality is obtained only transitorily, since before and after the collision only one lobe remains, the one for incidence before the collision and the one for transmission after the collision. As the collision progresses, the incident lobe decreases and the transmission one grows until they equilibrate and give the perfect cancellation and the two constructive interference zones of Fig. 1.

By changing the barrier height, the phases of the factors that multiply the w 's change, the lobules rotate with respect to each other, and one of the two in-phase regions grows while the other diminishes, so that the two peaks of the momentum distribution become asymmetric, see Figs. 3 and 4, where the momentum distributions and the corresponding lobules of the Argand diagrams are shown, compare also with Fig. 2. Note that these multiplying factors do not depend on time and therefore the angle between the lobules remains constant throughout the collision. This means that

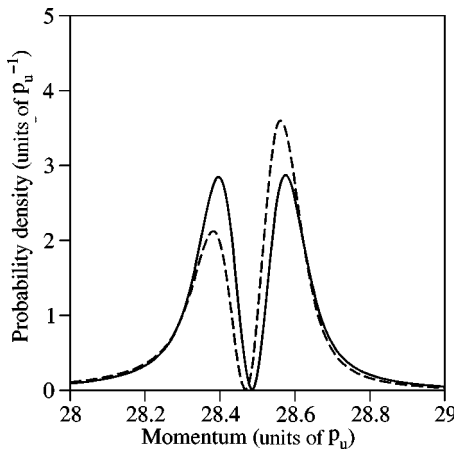


FIG. 3. $|\langle p|\psi(t)\rangle|^2$ as a function of p , for two different values of V_0 : $102.5e_u$ (solid line) and $105e_u$ (dashed line). The value of t is selected to get the maximum effect, $G^q=0.24$; $t=2.731t_u$. Other parameters as in Fig. 1.

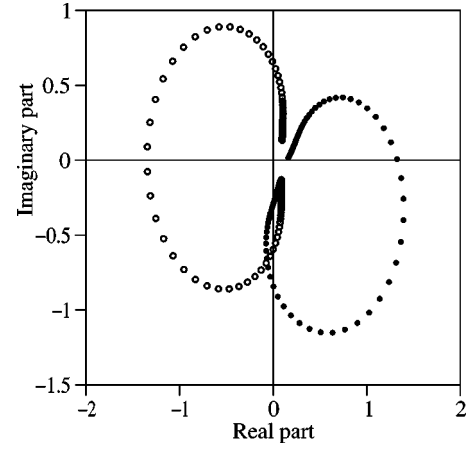


FIG. 4. Imaginary versus real parts of the incident contribution to $\psi_{IT}^0(p,t)$ (empty circles), and of the transmission contribution (filled circles), for $V_0=105e_u$, the value of t for which the effect is maximum ($t=2.731t_u$) and different values of p . Other parameters as in Fig. 1.

the positions of the maxima and minima of the momentum distribution do not change significantly for a given collision during the transient regime.

As stated before, the interference effect described does not depend on the square barrier-potential form and we have observed it in particular for a Gaussian barrier, chosen so that the truncation at $\pm d/2$ does not alter the scattering. Equation (11) is of general validity and independent of the potential shape, with $-d/2$ and $d/2$ being points where the potential may be assumed to be essentially zero. This is illustrated in Fig. 5, where both the exact distribution of momenta $|\langle p|\psi(t)\rangle|^2$, and the approximation $|\psi_{IT}^0(p,t)|^2$, are compared as a function of momentum for the Gaussian potential barrier.

The possibility to observe this effect with ultracold atoms rests on the ability to prepare appropriate initial states. Turn-

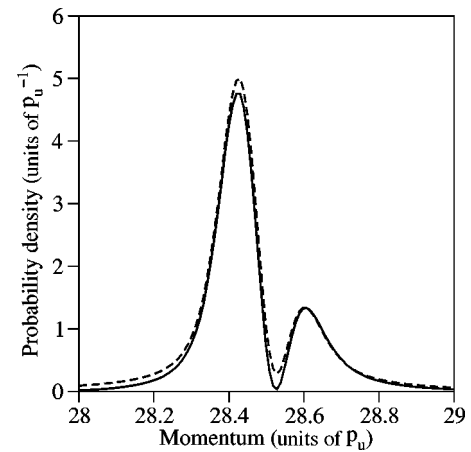


FIG. 5. Exact $|\langle p|\psi(t)\rangle|^2$ (solid line) and $|\psi_{IT}^0(p,t)|^2$ (dashed line) at time $t=2.68t_u$, during the collision of the same initial wave packet as in Fig. 1, against a Gaussian potential barrier of height $V_0=100e_u$, width $\sigma=1l_u$, and truncated at $\pm d/2$, where $d=9.6l_u$.

ing off the laser potential during the collision will leave a two-peaked momentum distribution that implies at later times a visible spatial separation between two wave components, one faster than the other.

We thank A. Steinberg for many useful discussions and acknowledge support by Ministerio de Ciencia y Tecnología (Grant No. BFM2000-0816-C03-03) and Gobierno Vasco (Grant No. PI-1999-28).

-
- [1] A. H. Zewail, *Femtochemistry* (World Scientific, Singapore, 1994).
- [2] R. F. Snider, *J. Stat. Phys.* **61**, 443 (1990).
- [3] S. Brouard and J. G. Muga, *Phys. Rev. Lett.* **81**, 2621 (1998).
- [4] S. Brouard and J. G. Muga, *Ann. Phys. (Leipzig)* **7**, 679 (1998).
- [5] D. H. Berman and R. F. Snider, *J. Chem. Phys.* **71**, 1740 (1979).
- [6] S. Brouard and J. G. Muga, *Phys. Rev. A* **54**, 3055 (1996).
- [7] G. W. Wei and R. F. Snider, *Phys. Rev. A* **52**, 2925 (1995).
- [8] *Handbook of Mathematical Functions*, edited by M. Abramowitz and I. A. Stegun (Dover, New York, 1972).
- [9] A. Pérez Prieto, Master thesis, Universidad de La Laguna, 2000.